



Article

Agricultural Drought Assessment in a Typical Plain Region Based on Coupled Hydrology–Crop Growth Model and Remote Sensing Data

Yuliang Zhang ¹, Zhiyong Wu ^{2,*}, Vijay P. Singh ^{3,4}, Juliang Jin ¹, Yuliang Zhou ¹, Shiqin Xu ⁵  and Lei Li ⁶

¹ School of Civil Engineering, Hefei University of Technology, Hefei 230009, China

² College of Hydrology and Water Resources, Hohai University, Nanjing 210098, China

³ Department of Biological and Agricultural Engineering, Texas A&M University, College Station, TX 77843, USA

⁴ National Water & Energy Center, UAE University, Al Ain 15551, United Arab Emirates

⁵ College of Geography and Environmental Science, Northwest Normal University, Lanzhou 730070, China

⁶ Tianjin Municipal Engineering Design & Research Institute, Tianjin 300000, China

* Correspondence: zywu@hhu.edu.cn

Abstract: An agricultural drought assessment is the basis for formulating agricultural drought mitigation strategies. Traditional agricultural drought assessment methods reflect agricultural drought degree by using the soil water deficit, e.g., Soil Moisture Anomaly Percentage Index (SMAPI). However, due to varying water demands for different crops, a given soil water deficit results in varying crop water deficits and agricultural droughts. This variation often leads to a misinterpretation of agricultural drought classification when one only considers the soil water deficit. To consider the influence of crop growth, this study proposes an agricultural drought assessment method by coupling hydrological and crop models (variable infiltration capacity–environmental policy integrated climate, VIC-EPIC). Agricultural drought in Jiangsu Province, China was evaluated using the VIC-EPIC model and crop water anomaly percentage index (CWAPI). The validation results based on the actual drought records showed that the correlation coefficients (0.79 and 0.82, respectively) of the statistical values and CWAPI simulated values of light and moderate drought area rates were greater than those for SMAPI (0.72 and 0.81, respectively), indicating that the simulation results of the VIC-EPIC model in Jiangsu Province were highly reasonable. The temporal and spatial variation characteristics of the drought grade in typical large-scale drought events in Jiangsu Province were also analyzed.

Keywords: agricultural drought assessment; VIC-EPIC; CWAPI; SMAPI; crop water demand; irrigation effects



Citation: Zhang, Y.; Wu, Z.; Singh, V.P.; Jin, J.; Zhou, Y.; Xu, S.; Li, L. Agricultural Drought Assessment in a Typical Plain Region Based on Coupled Hydrology–Crop Growth Model and Remote Sensing Data. *Remote Sens.* **2022**, *14*, 5994. <https://doi.org/10.3390/rs14235994>

Academic Editors: Guido D’Urso, Onur Yüzügüllü and Kyle Knipper

Received: 7 October 2022

Accepted: 17 November 2022

Published: 26 November 2022

Publisher’s Note: MDPI stays neutral with regard to jurisdictional claims in published maps and institutional affiliations.



Copyright: © 2022 by the authors. Licensee MDPI, Basel, Switzerland. This article is an open access article distributed under the terms and conditions of the Creative Commons Attribution (CC BY) license (<https://creativecommons.org/licenses/by/4.0/>).

1. Introduction

An agricultural drought assessment is the basis for formulating agricultural drought mitigation measures and preventing agricultural drought. Because the formation mechanism of agricultural drought is extremely complex and there are many influencing factors, it is difficult to build an effective agricultural drought evaluation method. Therefore, researchers have used drought indices to assess agricultural droughts.

Agricultural drought can be assessed based on the crop water deficit. A crop water deficit index (CWDI) has been proposed [1–3]. CWDI is the normalized difference [2,4,5] between the observed vegetative water consumption and water demand [6]. Consequently, CWDI can directly reflect the extent of agricultural drought and provide highly reliable results for assessing agricultural drought [7–9]. Accordingly, many studies [1–3,10] have conducted agricultural drought assessments based on CWDI. CWDI can be calculated using the following three methods:

(1) Remote sensing inversion

A remote sensing inversion method was proposed, along with the development of remote sensing technology [11–13]. This method was applied based on remote sensing data and estimation formulas (such as the energy balance method and crop coefficient method). The potential evapotranspiration and actual evapotranspiration were calculated as the crop water demand and water consumption, respectively. The CWDI [1,2,14,15] was obtained on this basis. This method considered the influence of the vegetation water content, and the estimation formula model's physical mechanisms. The CWDI was calculated using crop water demand, which was estimated using the potential evapotranspiration based on meteorological conditions alone; however, the influence of leaf area of crops in different growth periods on water demand was not considered [16–18]. Therefore, uncertainty regarding drought assessments based on remote sensing inversion remains.

(2) Crop growth model based on remote sensing data

With the continuous development of remote sensing technology, remote sensing data products have become increasingly mature. In the agricultural field, crop models are an important mathematical tool used to estimate the extent of crop water deficits. With the use of crop models to estimate the degree of water deficit, combined with remote sensing data products, the crop model is used to simulate the growth process of crops, and the CWDI is calculated to assess agricultural drought [19,20]. Wang, et al. [21] used microwave remote sensing to compute large-scale farmland soil moisture and calculated an agricultural drought index that reflected the degree of crop water shortage combined with crop models. The crop model improves the accuracy of regional agricultural drought assessments. However, some defects in microwave remote sensing data limit the accuracy of crop water consumption and the agricultural drought index simulated by crop models. The soil moisture of the surface layer (2–5 cm) can be retrieved through microwave remote sensing [22,23]; however, the soil moisture of the entire root layer of the crop cannot be calculated. The soil water content retrieved from remote sensing data has temporal discontinuities, owing to the long revisit periods of remote sensing satellites [24]. The significant soil moisture uncertainty can seriously affect the uncertainty of the water demand simulated by crop models and the resulting agricultural drought index based on crop water.

(3) Coupled hydrological crop-growth model

The simulation of soil water content using a hydrological model with a physical basis can consider the influence of vegetation and soil characteristics in different regions on the hydrological process. This is a more efficient method for obtaining spatially continuous soil profile water content data [25,26] and avoids temporal discontinuities in the retrieval of soil water content from remote sensing data. On this basis, a crop model was introduced which can consider the influence of dynamic changes in crop leaf area and water stress on the simulation of crop evapotranspiration and soil water content. This improves the simulation accuracy of soil water content. Combined with the advantages of accurate simulation of soil water content and evapotranspiration using the hydrological and crop models, the coupled hydrology–crop growth model improved the simulation accuracy of crop water consumption. In addition, the ability to identify agricultural drought with the coupled model was further improved compared with that with the single crop model.

Studies regarding the CWDI based on the coupled model have rarely been reported; however, related work has been reported. McNider, et al. [27] coupled the hydrology model of the water supply stress index (WaSSI) with the crop model of the decision support system for agrotechnology transfer (DSSAT). The CWDI, based on the crop water demand and water supply, was proposed for indicating crop water shortages, which showed patterns more similar to the actual drought conditions compared with other drought indices. However, the coupled model DSSAT-WaSSI could only simulate the growth of a single type of crop. Many types of crops are generally planted in a region's farmland. The variations in water consumption patterns of different crops may result in varying soil water

contents and crop water deficits. Consequently, it is difficult for DSSAT-WaSSI to accurately simulate and evaluate regional agricultural droughts. In addition, the irrigation module used in DSSAT-WaSSI did not consider the influence of limited water supply of the surface water body. The cultivated crops received more irrigation water than the model assumed, which would result in the simulated drought severity being less than the observed severity during drought periods. Hence, little attention has been paid to the construction of an agricultural drought index that considers the effects of different crops, the characteristics of different growth periods, irrigation, and crop rotation [28].

To overcome the issues of not considering the crop growth and irrigation in the agricultural drought assessment, the present study constructed the coupled hydrology–crop growth model called variable infiltration capacity–environmental policy integrated climate (VIC-EPIC), the proposed crop water anomaly percentage index (CWAPI) based on crop water demand, and consumption simulated by the VIC-EPIC model, and analyzed the index for regional agricultural drought assessment. The drought assessment results were compared with the soil moisture anomaly percentage index (SMAPI), which reflects the magnitude of soil water deficit. The comparison of the results was used to verify the viability of CWAPI.

2. Methodology

2.1. Framework of the VIC-EPIC Model

The two-way tightly coupled method was used to realize the coupling of EPIC and VIC models [29], and the soil water content calculated by the VIC model was passed to the crop model. The crop model simulated the crop growth process based on the soil water content, and the soil evaporation and crop transpiration calculated by the crop model were returned to the VIC model to calculate the initial soil water content for the next period.

Because crops require irrigation during the growth process, irrigation water from groundwater, rivers, and reservoirs is required. The calculation of water volume originating from rivers and reservoirs is inseparable from river routing; consequently, it was necessary to couple the routing module, reservoir module, and irrigation module with the VIC model. The routing model was the flexible large-scale hydrological routing model (FLASH) based on the merged grid [30], and sequential coupling was adopted between the VIC and the routing models. The VIC model passed the surface runoff and underground baseflow of each merged grid to the routing model, and the routing model was subsequently executed. Based on the runoff and routing models, an integrated coupling was used between the reservoir module and the routing model. The routing model transmitted the river flow data to the reservoir module, and the reservoir module performed the water balance calculation of the aggregated reservoir and simulated the water storage of the aggregated reservoir moment-by-moment [31]. The reservoir module returned the calculated discharge to the routing model. The irrigation module was coupled with a reservoir module. The irrigation module calculates the actual irrigation water based on the water storage value of the reservoir module, which supplements the actual irrigation water to the soil water content and passes the updated soil water content to the EPIC model. The construction principle of the VIC-EPIC model [32,33] is shown in Figure 1.

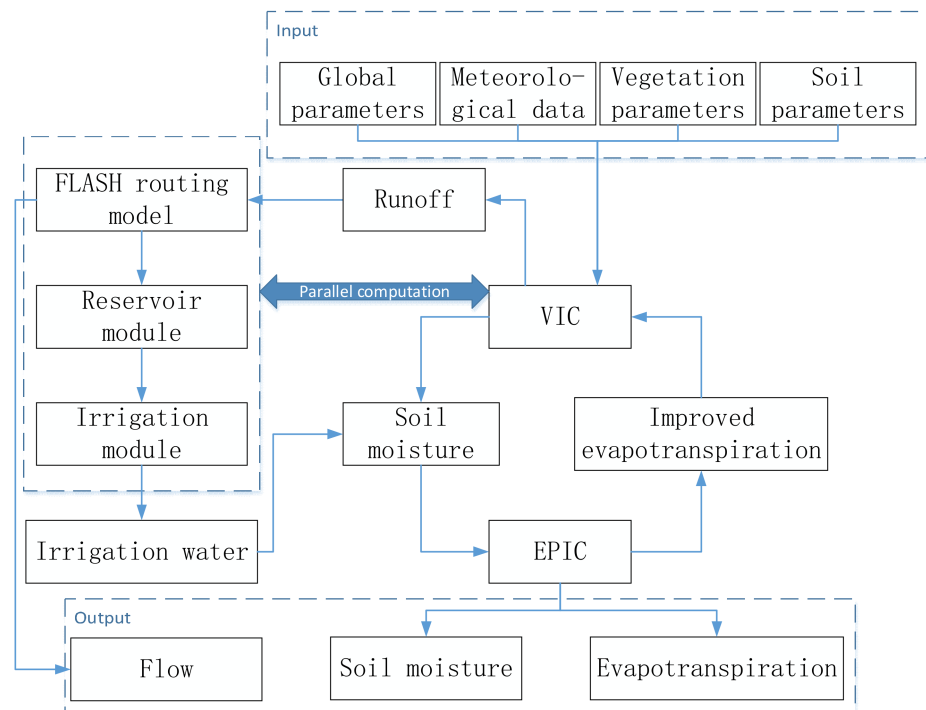


Figure 1. Flowchart of the coupled VIC-EPIC model integrated using FLASH and the reservoir module.

2.2. CWAPI

Based on the definition of agricultural drought (water deficit of crops caused by external environmental factors [34]), this study used crop water demand and water consumption to build a drought index reflecting the degree of crop water shortage. The crop water anomaly index (CWAI) was parameterized by:

$$CWAI_j = \left(\frac{E_{act,j} - E_{soil,act,j}}{E_j - E_{soil,j}} - 1 \right) \times 100\% = \left(\frac{E_{t,act,j}}{E_{t,j}} - 1 \right) \times 100\% \quad (1)$$

where $CWAI_j$ is the CWAI on a given day j (%); $E_{act,j}$ is the actual evapotranspiration on a given day j (mm); $E_{soil,act,j}$ is the actual soil evaporation on a given day j (mm); E_j is the potential evapotranspiration on a given day j (mm); $E_{soil,j}$ is the potential soil evaporation on a given day j (mm); $E_{t,act,j}$ is the actual transpiration of crops on a given day j , i.e., crop water consumption (mm); and $E_{t,j}$ is the maximum crop transpiration on a given day j , i.e., crop water demand (mm).

The CWAPI was constructed to describe the CWAI in each region with a unified standard, based on the Formula (2) to assess agricultural drought [1,34].

$$CWAPI = \frac{CWAI_i - \overline{CWAI}}{100 + \overline{CWAI}} \times 100\% \quad (2)$$

where $CWAPI$ is the CWAPI in some periods, $CWAI_i$ is the weighted average of the CWAI for a given period i (%), see Formula (3)), and \overline{CWAI} is the contemporaneous average of the CWAI in the calculated period, which is 30 years in this study (see Formula (4)).

$$CWAI_i = k_1 \times CWAI_j + k_2 \times CWAI_{j-1} + \dots + k_{50} \times CWAI_{j-49} \quad (3)$$

where $CWAI_i$ is the weighted average of the $CWAI$ for a given period i (%), $CWAI_j$ is the $CWAI$ on a given day j (%), and k_j is the weight coefficient of $CWAI_j$ [34].

$$\overline{CWAI} = \frac{1}{n} \sum_{m=1}^n CWAI_m \quad (4)$$

where n is the total number of analyzed years, generally more than 30, and m is the serial number of each year, $m = 1, 2, \dots, n$.

To formulate a reasonable drought level classification standard, based on the research ideas of Wu, et al. [35], Mao [36], and Palmer [37], the CWAPI frequency distribution in the study area was calculated. Drought was then classified based on the frequency distribution and frequency of different drought levels reported by Mao [36] and Wu, et al. [35] (see Table 1). To consider the influence of different growth periods of crops on the agricultural drought levels, referring to the treatment method for the critical period of crop water demand in “Grade of Agricultural Drought” [34], the droughts of the critical period of crop water demand and other growth periods were classified.

Table 1. Agricultural drought grades based on CWAPI.

Drought Levels	CWAPI/%	
	Other Growth Stages	Critical Period of Crop Water Demand
Light drought	(−10, −30]	(−5, −25]
Moderate drought	(−30, −40]	(−25, −35]
Severe drought	(−40, −45]	(−35, −40]
Extremely drought	(−45, −∞)	(−40, −∞)

In this study, the droughts characterized by CWAPI and SMAPI are referred to as crop drought and soil drought, respectively. SMAPI is often calculated using the soil water content simulated by the VIC model [35,38]. Because the VIC model failed to simulate irrigation and crop growth processes, and the simulated soil water content was the average soil water content for all land-use types, the VIC-based SMAPI was not affected by crop growth and irrigation. In this study, the SMAPI dryness and wetness scale suggested by Lu, et al. [39] was used (Table 2).

Table 2. Drought and flood grades of SMAPI.

SMAPI	Grade	SMAPI	Grade
$SMAPI \leq -25\%$	Extreme drought	$5\% < SMAPI \leq 10\%$	Light flood
$-25\% < SMAPI \leq -20\%$	Severe drought	$10\% < SMAPI \leq 15\%$	Moderate flood
$-20\% < SMAPI \leq -15\%$	Moderate drought	$15\% < SMAPI \leq 25\%$	Severe flood
$-15\% < SMAPI \leq -5\%$	Light drought	$SMAPI > 25\%$	Extreme flood
$-5\% < SMAPI \leq 5\%$	Normal state		

Recently, drought has occurred frequently in Jiangsu Province. SMAPI was built using soil water content simulated by the VIC model to identify drought events in Jiangsu Province, China. CWAPI was built on this basis, and the drought characteristics and changing laws of agricultural drought events in Jiangsu Province were investigated. These have an important role in understanding the occurrence and development processes of drought in Jiangsu Province and may provide a basis for large-scale drought monitoring and prediction.

2.3. Validation Method

Currently, there is a scarcity of the measured drought index data, and only the drought-related statistics and other widely used drought indices and their related hydrological variables can be used to validate the rationality of the calculated results of the drought index.

The observed soil moisture and statistical data on the drought area each year are compared with the simulation results of VIC-EPIC. Using Equations (5)–(8) (percent bias, PBIAS; normalized root mean square error, NRMSE; root mean square error, RMSE), the rationality of CWAPI can be validated. Comparisons with other verified drought indices can also indicate if the proposed drought indices are reasonable. Studies have proposed other agricultural drought indices that have been verified using observational data. For example, Wu, et al. [35] and Mao, et al. [38] applied the SMAPI drought index to agricultural drought assessments in China and Jiangsu Province, respectively, and noted the applicability to be good. Therefore, this study compared the change process of SMAPI and CWAPI, found the difference between the change processes, and used the drought formation process to show that the difference is more reasonable for verifying the feasibility of CWAPI.

$$PBIAS = \left(\frac{\sum_{t=1}^T (f_t - y_t)}{\sum_{t=1}^T y_t} \right) \times 100 \quad (5)$$

$$NRMSE = \sqrt{\frac{1}{T} \times \sum_{t=1}^T (f_t - y_t)^2} \times \frac{100}{\bar{y}} \quad (6)$$

$$R = \frac{\sum_{t=1}^T (f_t - \bar{f})(y_t - \bar{y})}{\sqrt{\sum_{t=1}^T (f_t - \bar{f})^2 \sum_{t=1}^T (y_t - \bar{y})^2}} \quad (7)$$

$$RMSE = \sqrt{\frac{1}{T} \times \sum_{t=1}^T (f_t - y_t)^2} \quad (8)$$

where f_t is the simulated value of the model at time t , $t = 1, 2, \dots, T$; y_t is the observed value at time t ; \bar{f} is the average value of the simulated value of the model at all times; and \bar{y} is the average value of the observed value at all times.

2.4. Study Area and Data

Jiangsu Province is in the Jianghuai region of eastern China and has a total area of 107,200 square kilometers, spanning across 30°45′–35°08′ north latitude and 116°21′–121°56′E longitude, bordering Shanghai, Zhejiang, Anhui, and Shandong. Jiangsu is a coastal area across a river, with many lakes and a flat terrain. The landform consists of plains, water, low mountains, and hills. It faces the Yellow Sea to the east and crosses the Yangtze and Huaihe Rivers. Jiangsu geographically spans the north and south, and its vegetation and climate have characteristics of both areas. The annual average temperature varies between 13 °C and 16 °C, and the average annual precipitation is approximately 1000 mm. It consists of more than 8000 watersheds. However, the temporal and spatial distribution of precipitation in Jiangsu Province is uneven, and regional differences are significant. It is a typical area in China with frequent droughts and floods [40]. During recent years, large-scale and high-impact drought events have continuously occurred under the combined influence of climate warming and human activities. For example, Jiangsu Province suffered a severe drought in 2011, and Shijiu Lake in Nanjing City was almost dry. In 2016, Hongze Lake was dry for a long period, which brought great inconvenience to water transportation in the lake area. Changzhou also experienced continuous high temperatures and dry weather, which severely restricted the development of local agriculture. From mid-September to December 2019, the average rainfall in Jiangsu Province was 91 mm, which was 48% less than that during the same period of the previous year. Most of the province was in moderate or above meteorological drought, and the regions toward the south of the Huaihe River experienced

severe drought. Jiangsu Province is a province with high gross domestic product (GDP), ranking fourth in terms of total agricultural output value in 2019 among 31 provinces. The frequent occurrence of droughts has remarkably affected the normal progress of local agricultural production and has become an important factor in restricting the economic and social development of Jiangsu Province.

The VIC-EPIC model was constructed for Jiangsu Province to study the formation of local agricultural drought. The meteorological data used in the model are the 6-h-scale data of a 5 km merged grid obtained by the inverse distance weight interpolation method based on the daily dataset from the China Meteorological Data network [41]. The spatial distribution of crops was detected based on moderate resolution imaging spectroradiometer (MODIS) remote sensing products, as shown in Figure 2. DEM data were obtained from the shuttle radar topography mission (SRTM) [42] with a resolution of 30 m. The water area data originate from the 30 m resolution water data product developed by the European Commission Joint Research Center [43]. The soil parameters in the VIC model were calculated based on the soil database [44] and soil characteristic parameter formula of Saxton [45]. The property parameters of the different types of crops came from the crop parameter library of the SWAT model. The parameters of the hydrological model were calibrated and transferred using measured hydrological data [25,36,46,47].

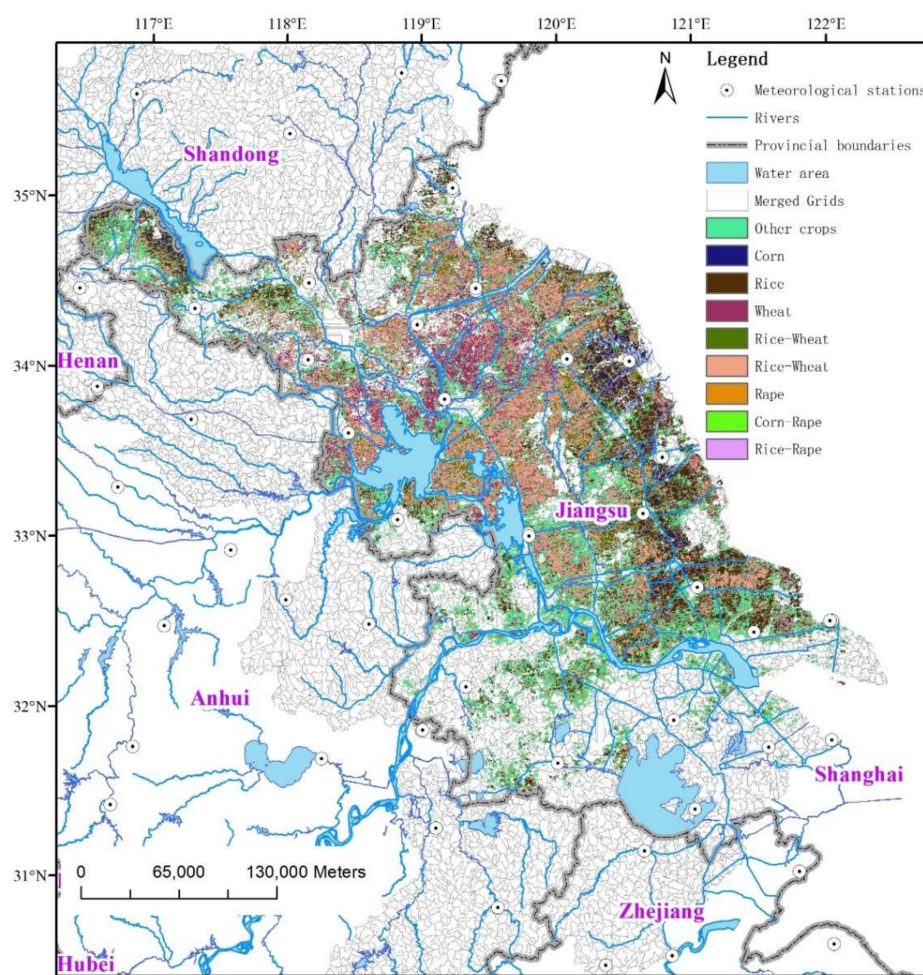


Figure 2. Spatial distribution diagram of meteorological stations, water area, and crop rotation types in Jiangsu province.

3. Results

3.1. Validation Based on Soil Moisture

To validate the VIC-EPIC simulation results, this study used data from 99 soil moisture stations in Jiangsu Province's watersheds to calculate the correlation coefficient, the soil water content's PBIAS, RMSE, and NRMSE between the soil moisture simulation and observation at a depth of 10 cm. Figure 3 shows that the percentage of soil moisture sites with a correlation coefficient greater than 0.60 accounted for 25%, and the average correlation coefficient was 0.40, which was higher than that noted in prior studies [12,48].

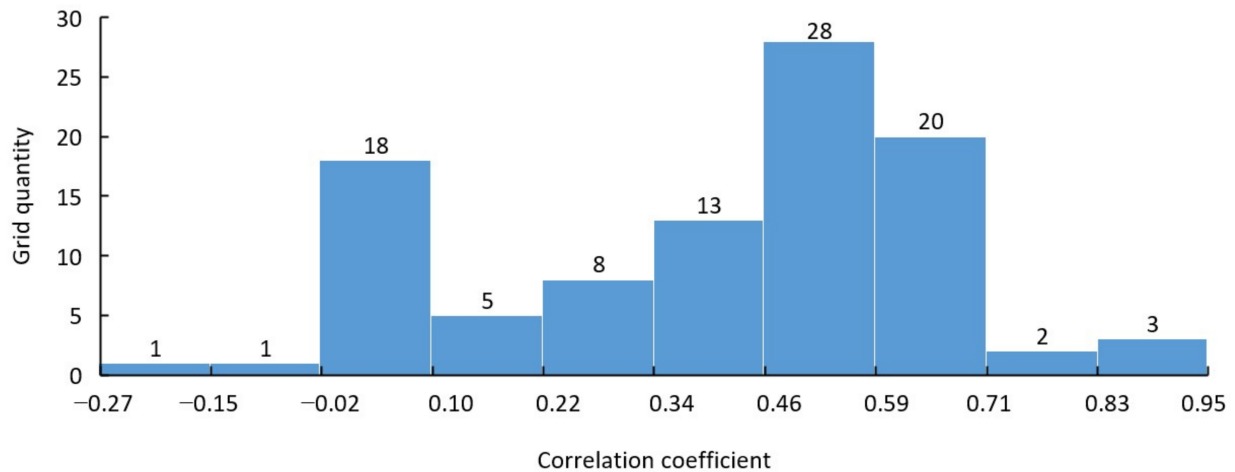


Figure 3. Frequency histogram of correlation coefficients between 10 cm soil moisture of simulation and observation in merged grids containing soil moisture stations of Jiangsu province.

Figure 4 shows that the simulation accuracy in the north was generally better, but there was no trend in the spatial distribution of errors. The soil water content and evapotranspiration at some stations were well simulated, particularly when the RMSE was used as the error index. There were some points close to the river channel where the soil water content simulation accuracy was greater, which may be related to the model considering irrigation because the area close to the river was generally within the effective irrigation area.

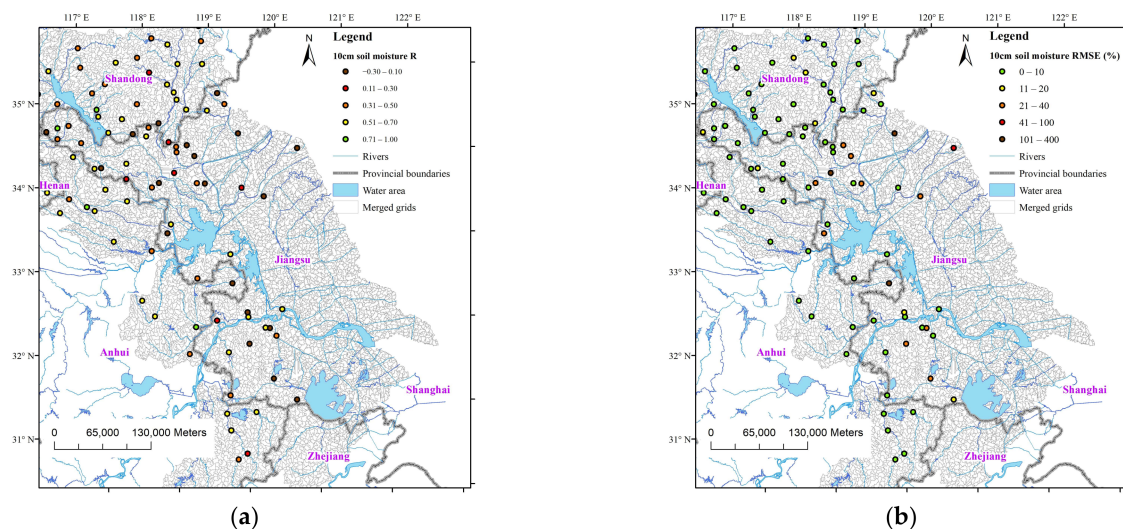


Figure 4. Cont.

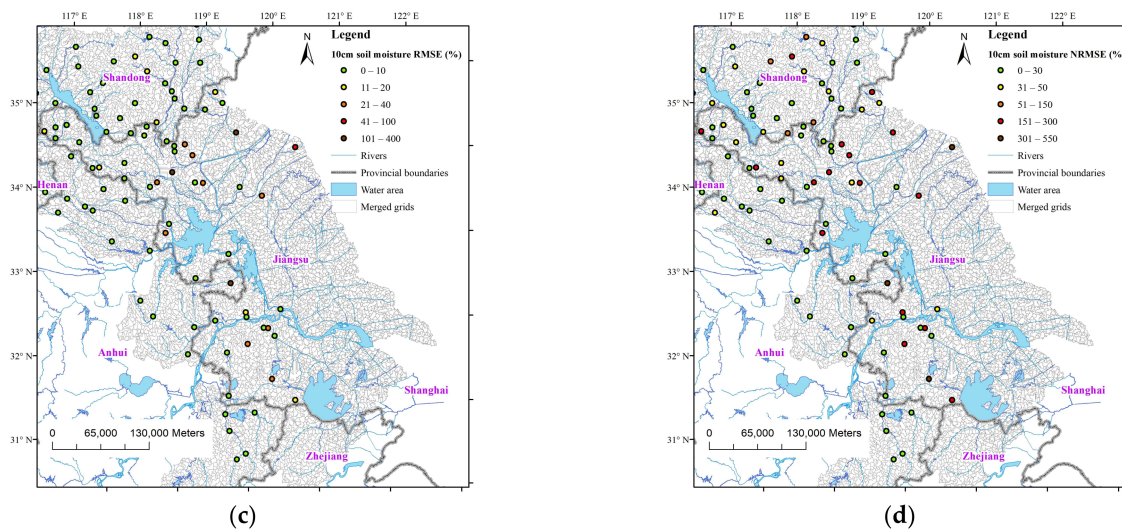


Figure 4. Soil moisture error indices at 10 cm depth, as per the VIC-EPIC model and ground stations in Jiangsu province. (a) Correlation coefficient; (b) PBIAS, percent bias; (c) RMSE, root mean square error; (d) NRMSE, normalized root mean square error.

3.2. Validation Based on the Drought Record

Because the water absorbed by crop roots comes from the soil at a depth of 0–40 cm [49–51], the default soil water content used in the SMAPI constructed in this study was the average soil water content at a depth of 0–40 cm for all land use types calculated by the VIC-EPIC model [35,38].

The drought area rate corresponding to each year's drought index in Jiangsu Province was calculated and compared with the statistical drought-affected area rate recorded in yearbooks [52]. The correlation coefficients (0.79 and 0.82) between the statistical values of the drought-related area rate and light and moderate drought area rate calculated based on CWAPI were greater than those (0.72 and 0.81) for SMAPI. This indicates that the drought results based on the VIC-EPIC model simulation were reasonable and feasible, and CWAPI could reflect agricultural drought characteristics more reasonably at a regional level.

Figure 5 shows that the variation trend of the simulated drought area rate from 2011 to 2013 was very close to the statistical variation trend of the drought-affected area rate. A comparison of the bar graphs of the area rates of different drought grades year-by-year showed that the greater the drought grade, the smaller the corresponding drought area rate, and the relationship between years varied. For example, the light drought area rate in 2012 was smaller than that in 2014, whereas the severe drought area rate in 2012 was greater than that in 2014, and the relative relationship between the severe drought area rate and the statistical value of the drought-affected area rate was more consistent. This was related to the fact that the statistical value of the drought-affected area rate was calculated based on the record data of yield loss area, and the water deficit of severe drought was larger than that of light drought, which made severe drought more likely to cause yield loss. Hence, the variation trend of the area rate of severe drought showed a pattern more similar to that of the statistical drought-related area rate compared to that of the light drought.

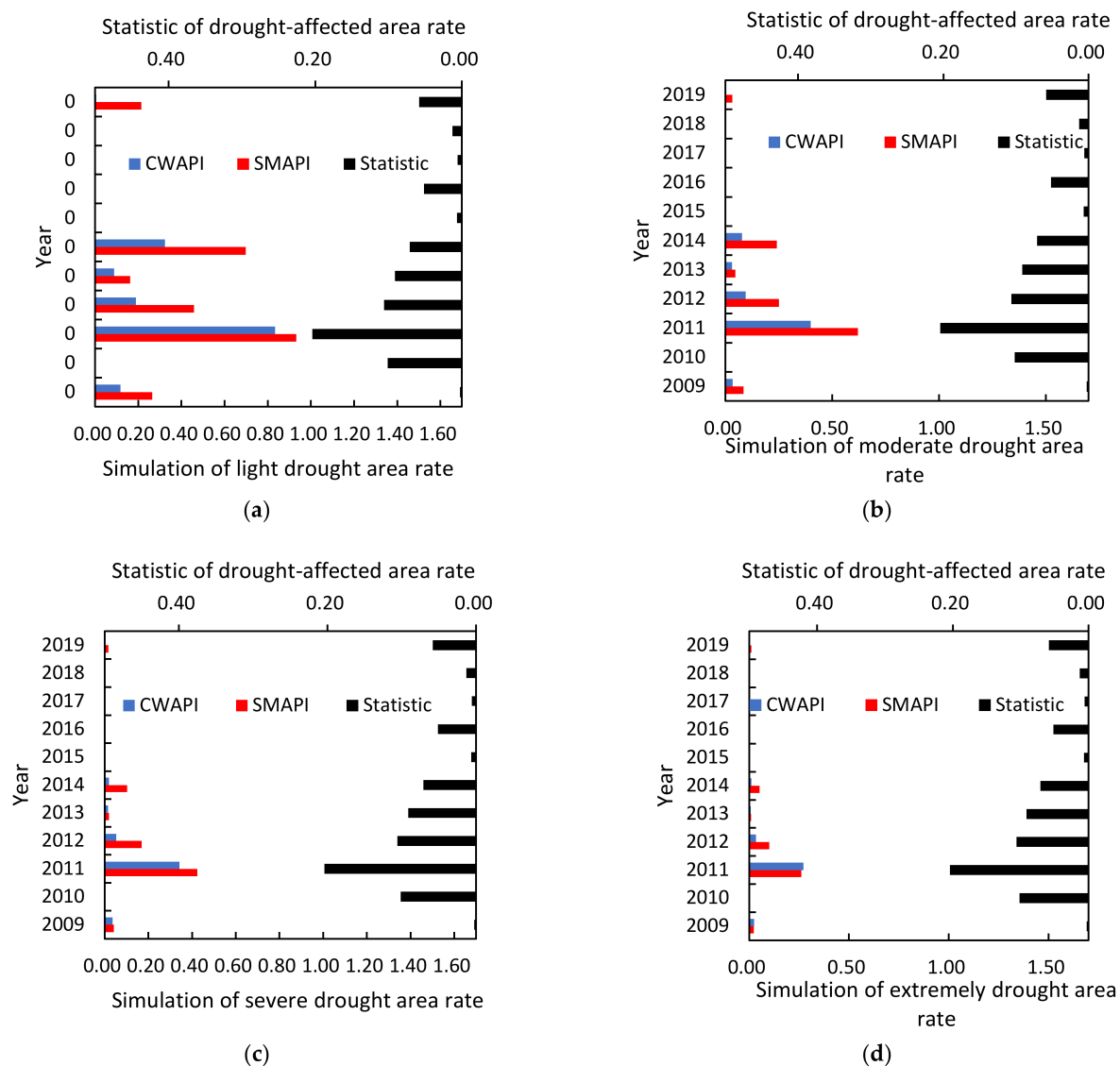


Figure 5. Bar diagrams of the statistical values of drought-affected area rates and the area rates of different drought grades in Jiangsu Province from 2009 to 2019 (a–d correspond to light, moderate, severe, and extremely drought area rates, respectively).

The actual drought of the year was recorded in the annual “Jiangsu Water Conservancy Yearbook” [52]. CWAPI simulation results based on the VIC-EPIC model were verified using drought records. According to a previous study [52], in 1989, the rainfall in Jiangsu Province was 20% less than that of normal years during the flood season, and the rainfall at the time of sowing was only 14 mm. Most of the small- and medium-sized reservoirs dried up, the soil moisture content of the cultivated layer was only 5%, and 16 million mu (1 mu = 0.0667 ha) was fully affected by drought. In 1992, a severe drought occurred in northern Jiangsu and hilly and mountainous areas during the flood season. From July to August, the drought affected the entire province. Drought severity in some areas exceeded that of 1989. This was the driest year since 1978. More than 30 million mu of the province has suffered from drought. In 1998, there was little rainfall after the flood season, and a severe autumn drought occurred on the coast and in the hilly and mountainous areas of northern and southern Jiangsu. The drought-affected area is as large as 20 million mu. In 2010 and 2011, continuous droughts occurred in autumn, winter, spring, and summer, with serious soil moisture shortages and abnormally dry inflows. There was a large drought-affected area of 4.3663 million mu. Overall, severe droughts occurred in 1989, 1992, 1998,

and 2011. The drought-affected area in 1992 was the largest during these four years, but the assessment results based on SMAPI did not reflect this conclusion. The assessment results based on CWAPI showed that the drought in 1992 was the most severe of these four years. Hence, CWAPI is more suitable than SMAPI for characterizing severe agricultural droughts. Sayago, et al. [53] also found that the correlation between the remote sensing drought index and ET_c/ET_0 was superior between the remote sensing drought index and the soil water deficit, indicating that CWAPI based on ET_c/ET_0 was more suitable for characterizing agricultural drought than SMAPI.

4. Discussion

4.1. Temporal and Spatial Variation Process of Large-Scale Drought

4.1.1. Analysis of the Change Process in the Drought Grade Area and Typical Prefecture-Level Drought Index

From mid-September to December 2019, the average rainfall in Jiangsu Province was 91 mm, which was 48% less than what was recorded in the same period of the previous year, and severe meteorological drought occurred. Most of the province was in moderate or above meteorological drought, and the areas toward south of the Huai River were in severe drought. To analyze the change process of this drought, the change in the area ratio of different drought grades in Jiangsu Province in 2019 was plotted.

Figure 6a shows that the proportion of moderate drought areas, calculated based on SMAPI, was generally larger than that based on CWAPI, which was related to the ability of the crop drought index to intensify the effects of irrigation, water demand, and fallow during agricultural drought. (1) Irrigation water quantity had a greater impact on drought relief, as indicated by CWAPI, than indicated by SMAPI. As a result, the drought severity indicated by CWAPI was less than that indicated by SMAPI. For example, during the flood season from June to October, there was more precipitation and the water storage of the aggregated reservoir was significant. The crop water demand was elevated when there was high temperature and no rain in summer, resulting in a large volume of irrigation water during this period (see Figure 6b). Therefore, the proportion of moderate drought areas in Jiangsu Province, indicated by CWAPI, was less than that indicated by SMAPI. (2) In the early stages of growth and near maturity, the water demand of crops is typically low. Currently, crops require less water to maintain normal growth. Therefore, the degree of drought indicated by CWAPI was less than that indicated by SMAPI. For example, in March-April and October-November, crops required less water in the early stages of growth; consequently, drought formation rarely occurred during these periods. (3) Crop fallow was also one of the reasons for the low proportion of dry areas in CWAPI. For example, in early June and mid-October, farmland lay fallow; consequently, the proportion of moderate drought areas during this period was close to zero. The crop model used to calculate crop water consumption in CWAPI also considers the effect of crop drought tolerance. Wheat and maize had stronger drought tolerance performance; thus, slight water shortages had less inhibition of their growth, and the drought degree of crops represented by CWAPI was low. (4) When calculating SMAPI, the leaf area index (LAI) used by the VIC model kept a constant value for each month, which could not consider the effect of the small LAI of vegetation in the early stage of growth. Consequently, the crop water consumption was greater and the soil water content was lesser, which also made the proportion of moderate drought area of SMAPI relatively large. Overall, five factors, irrigation, crop water requirements, and fallow, made the proportion of moderate drought areas calculated based on SMAPI greater than that calculated based on CWAPI.

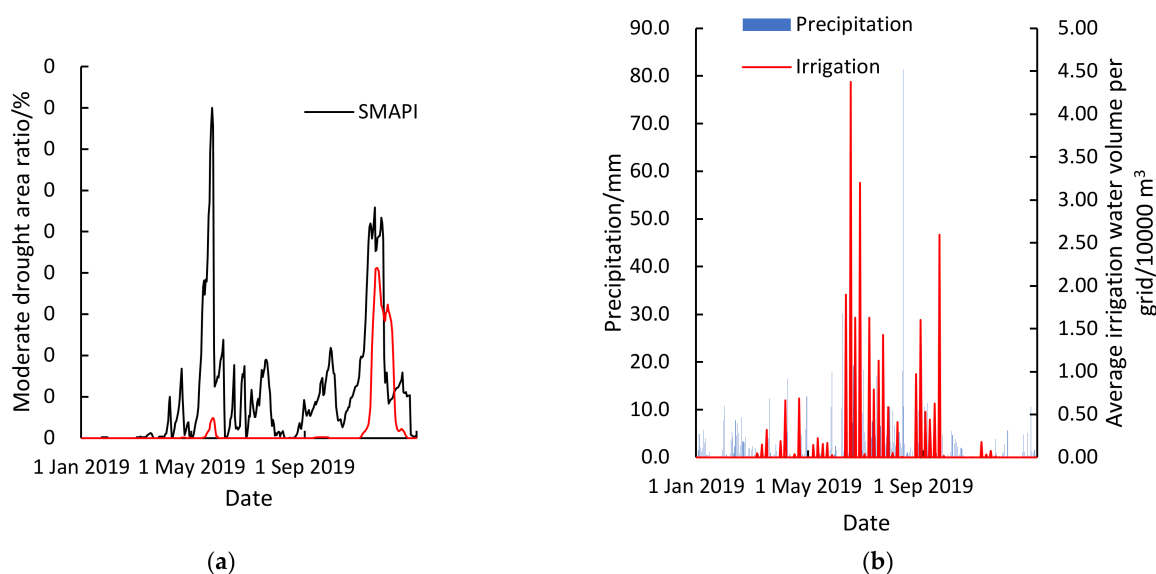
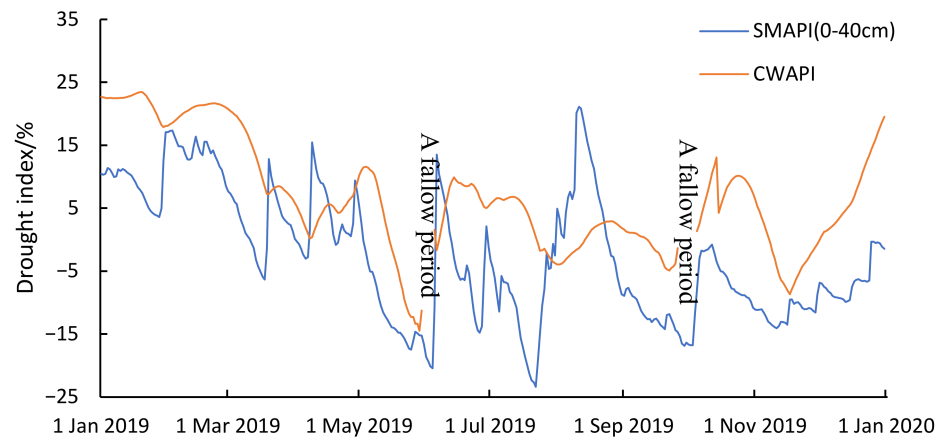


Figure 6. (a) Time courses of the area ratio of the moderate drought grade calculated by SMAPI and CWAPI; (b) Time courses of precipitation and irrigation of Jiangsu Province in 2019.

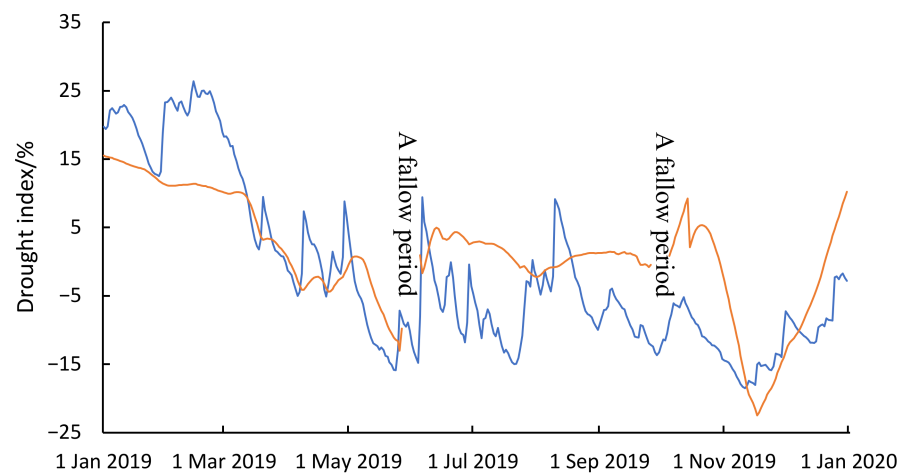
Figure 6a shows that there were two large extreme values of the area ratio of moderate drought on 22 May 2019 and 19 November 2019. By reviewing news reports, it was found that there were no reports of drought in May 2019; however, there were some reports of drought in November 2019. For example, Jiangsu reported on November 19 [54] that the drought-affected area of wheat in the province reached 2.63 million mu. The drought during November was more serious than that during May, which was consistent with the change in the proportion of moderate drought areas reflected by CWAPI; however, the simulation results of SMAPI showed that the light drought area ratios on 22 May and 13 November were both greater than 0.25, and the ratio of the drought-affected area in May was even larger than that in November, which was inconsistent with the actual events.

Taking typical drought-prone areas in Jiangsu Province as examples, such as Xuzhou City, Lianyungang City, and Huai'an City, the rationality and change process of the drought index in 2019 were analyzed. In terms of the rationality analysis, Figure 7 shows that the drought in Huai'an was the most severe, followed by Xuzhou and Lianyungang. The statistical results showed that the drought-affected area rates of Huai'an, Xuzhou, and Lianyungang were 24%, 11%, and 5%, respectively. Therefore, the CWAPI simulation results were consistent with the statistical results for the 2019 drought-affected area rate.

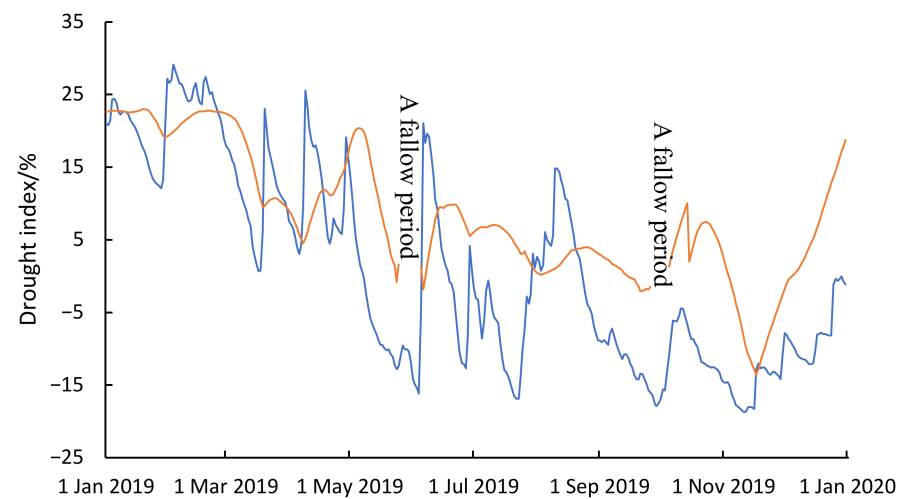
The process of change of the drought index in Xuzhou, Lianyungang, and Huai'an showed both similarities and differences. Figure 7 shows that the similarities of changes in the drought index of each city were as follows: the change in the crop drought index had a certain lag relative to that of the soil drought index; and the crop drought index changed slowly because of slow growth. There were also significant differences in the index change process of each city; the SMAPI in Lianyungang City was relatively elevated during the first half of the year, which was related to the large volume of irrigation water in the city, but CWAPI was more easily affected by irrigation, which resulted in greater distance between the CWAPI and SMAPI lines in Lianyungang City during May 2019 compared to that of Xuzhou and Huai'an. In the second half of the year, the smaller SMAPI and CWAPI were related to smaller precipitation. The CWAPI of Huai'an was generally small, which is related to its latitude. The temperature in Huai'an was greater than that in Xuzhou and Lianyungang, which led to high evapotranspiration. The irrigation water per unit area of Huai'an was also relatively small; the two factors of evapotranspiration and irrigation water decreased the soil water content, and the crops were susceptible to water stress. Therefore, the CWAPI in Huai'an City were small.



(a) Xuzhou City



(b) Huai'an City



(c) Lianyungang City

Figure 7. Time series of drought indices of Xuzhou (a), Huai'an (b), and Lianyungang (c) in 2019.

4.1.2. Analysis of Changes in Spatial Distribution of Large-Scale Drought Levels

In the first half of 2000, a severe drought occurred in Jiangsu Province, resulting in a drought-affected area rate of 0.239 and a disaster-affected area rate of 0.171. The disaster level during the 32 years from 1985 to 2016 was less than that in 1988 and 1994. To analyze

the formation process of drought events, the level distribution map of the drought index on 9 February, 18 April, 10 May, 25 May, and 3 June 2000, are shown in Figure 8.

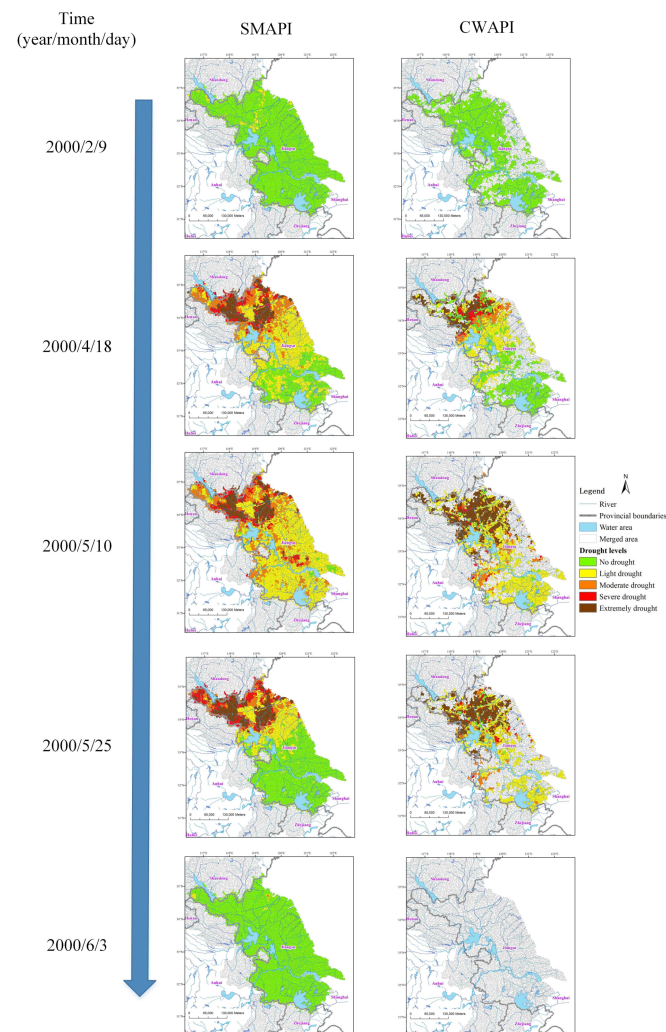


Figure 8. Spatial distribution of drought levels using SMAPI and CWAPI on 9 February, 18 April, 10 May, 25 May, and 3 June 2000 in a large-scale drought event in Jiangsu Province.

The soil drought event began in early February, and by mid-April, it spread across the central and northern parts of Jiangsu Province. Some parts of the northern region were subject to severe and extreme drought conditions. In early May, the drought spread to the entire Jiangsu Province, and the drought in the northern part remained severe. Compared with the drought in mid-April, the coverage area of severe and extreme droughts in early May remained unchanged, and the area of moderate drought expanded. During late May, the drought event in the south ended, and the drought in the north continued, but the severe and moderate droughts in some regions were degraded to moderate and light droughts, respectively, while the areas covered by extreme drought remained unchanged. Finally, drought in Jiangsu Province was relieved at the beginning of June. The development process of drought events indicated that it took a long time for a soil drought event to develop into a provincial drought, whereas it took a short time to recover from a provincial drought to a normal state, which was determined by large-scale and long-term precipitation in Jiangsu Province during late May. Therefore, the large-scale soil drought event in Jiangsu Province in 2000 was characterized by slow development and rapid relief.

Crop drought events began to occur in the first ten days of April and developed to the north of Jiangsu Province during mid-April. Extreme drought and severe drought

occurred in some regions of northern Jiangsu Province. By the first ten days of May, the drought-related area became larger, and the degree of drought increased. The drought levels in some regions changed from severe and light drought to extreme drought. Since late May, the degree of drought in some regions had eased, and the drought-related area had decreased. The drought level in some regions near the middle of Jiangsu Province reduced from extreme to moderate. Finally, the crop drought in the entire province ceased by early June. As a result, the large-scale crop drought event in Jiangsu Province in 2000 also had characteristics of slow development and rapid relief.

There were similarities and differences regarding the development processes of soil drought and crop drought. In terms of similarities, the spatial and temporal trends of soil drought and crop drought were similar, both of which were severe drought in the north and moderate drought in the south. Both gradually spread from the north to most regions of the province. The consistency of the distribution and change trends of the two drought indices indicated that the proposed CWAPI was reasonable. In terms of differences, the drought-related areas of crops were smaller than those of the soil droughts. For example, in the first ten days of May, the soil drought spread to the whole province, while the crop drought did not occur in the middle and east of Jiangsu Province and was affected by the crop fallow period. The assessment scope of agricultural drought did not include the area of the central and southern Jiangsu Province. The crop drought duration was shorter than that of soil drought. Soil drought had occurred since the first ten days of February, while crop drought had gradually occurred since the first ten days of April. Therefore, the severity of soil drought was obviously more serious than that of crop drought because the CWAPI (based on VIC-EPIC) considered the impact of slow growth and water demand of crops and was more affected by irrigation than SMAPI. Although the drought level of crops in most regions was less than that of soil, the drought level of crops in some regions was higher than that of soil. For example, this phenomenon occurred in some regions in the Huaihe River Basin in the north of Jiangsu Province in early May 2000, which was related to the drought level of CWAPI, considering the critical period of crop water demand. Table 1 shows that the drought level of some CWAPIs in the critical period of water demand was more severe than that in the other periods.

5. Conclusions

Based on CWAPI, an agricultural drought assessment was performed over a large area to consider the influence of crop growth and irrigation. From one perspective, Jiangsu Province was used as the research area, the VIC-EPIC model was constructed, and CWAPI was established based on the simulated crop water demand and consumption, which validated the application of CWAPI in Jiangsu Province. From the other perspective, combined with the difference of underlying surface, the spatio-temporal change in agricultural drought was evaluated. The following conclusions were obtained:

- (1) A VIC-EPIC model was constructed in Jiangsu Province, and the simulation results of the VIC-EPIC model and evaluation results of the CWAPI drought index were verified. The soil moisture results of the VIC-EPIC model were verified using 99 moisture-site data. The average correlation coefficients between the soil moisture of the simulation and observation at the 25% soil moisture stations were greater than 0.60, indicating that the simulation results of the VIC-EPIC model were very reasonable.
- (2) The correlation coefficients (0.79 and 0.82) between the statistical values of the drought-related area rate and light and moderate drought area rate calculated based on CWAPI were greater than those (0.72 and 0.81) for SMAPI. The drought characteristic values based on CWAPI showed better agreement with the more severe drought events recorded. The drought results based on the VIC-EPIC model simulation were reasonable and feasible, and CWAPI could reflect agricultural drought characteristics more reasonably at a regional level.
- (3) The drought reflected by CWAPI in Jiangsu Province during November of 2019 was much more severe than that during May, which was consistent with the data

regarding the actual drought-affected area, while the drought reflected by SMAPI was the opposite. The drought-affected area rate of Huai'an, Xuzhou, and Lianyungang in 2019 was 24%, 11%, and 5%, respectively. The CWAPI simulation results were consistent with the statistical results of the 2019 drought-affected area rate. Therefore, the CWAPI can reveal the drought characteristics with greater reliability.

- (4) In the large-scale drought of 2000, the severity of soil drought was significantly greater than that of crop drought because the crop drought simulation was more influenced by irrigation; the spatial and temporal trends of soil drought and crop drought in 2000 were similar.

This study analyzed crop water demand and crop water consumption, constructed the CWAPI, and, finally, explained the regional agricultural drought characteristics. However, as a result of agricultural drought process complexity, there are aspects that still need to be improved. For example, at present, many remote sensing data products are closely related to drought assessment, such as MODIS LAI and MODIS ET. The use of these data to improve the simulation accuracy of the VIC-EPIC model requires further investigation. In addition, if crop water shortage can be directly converted into drought-related yield reduction, the yield reduction as an agricultural drought index would have a clearer physical significance, directly reflecting the impact of drought on agricultural production. Agricultural drought assessment based on remote sensing data and yield reduction simulations is the key direction of our research group.

Author Contributions: Writing—original draft, Y.Z. (Yuliang Zhang); data curation, Z.W.; investigation, Y.Z. (Yuliang Zhang); methodology, Y.Z. (Yuliang Zhang) and Z.W.; calculation, Y.Z. (Yuliang Zhang); supervision, Z.W. and J.J.; validation, Y.Z. (Yuliang Zhang) and Y.Z. (Yuliang Zhou); writing—review and editing, V.P.S., S.X. and L.L. All authors have read and agreed to the published version of the manuscript.

Funding: This work was financially supported by the National Natural Science Foundation of China (52209011, U2240225), the Anhui Provincial Natural Science Foundation (2208085QE179, 2108085QE254), the Fundamental Research Funds for the Central Universities (JZ2022HGQB0213, JZ2021HGTA0165), the National Natural Science Foundation of China (42271084, U2240223, 52109009), Belt and Road Special Foundation of the State Key Laboratory of Hydrology-Water Resources and Hydraulic Engineering (2020490711).

Data Availability Statement: The data that support the findings of this study are available from the corresponding author, upon reasonable request.

Conflicts of Interest: The authors declare that they have no conflict of interest.

References

1. Jackson, R.D.; Idso, S.B.; Reginato, R.J.; Pinter, P.J. Canopy temperature as a crop water stress indicator. *Water Resour. Res.* **1981**, *17*, 1133–1138. [[CrossRef](#)]
2. Wang, Y.J.; Wang, S.D.; Zeng, H.J.; Cai, M.Y.; Song, W.L. Drought characteristic in the Weihe river basin based on water shortage index of crops. *Arid Zone Res.* **2014**, *31*, 118–124. (In Chinese with English Abstract)
3. Liu, A.; Li, X.; He, Y.; Deng, F. Simplification of crop shortage water index and its application in drought remote sensing monitoring. *Chin. J. Appl. Ecol.* **2004**, *15*, 210–214. (In Chinese with English Abstract) [[CrossRef](#)]
4. Shi, X.; Li, F.; Yan, B.; Dong, H.; Duoji, P.; Zhen, Q. Effects of water deficit on water use and yield of spring highland barley under straw mulching. *Trans. Chin. Soc. Agric. Eng.* **2016**, *S1*, 105–111. (In Chinese with English Abstract)
5. Huang, J.; Li, L.; Zhang, C.; Yun, W.; Zhu, D. Evaluation of cultivated land irrigation guarantee capability based on remote sensing evapotranspiration data. *Nongye Gongcheng Xuebao/Trans. Chin. Soc. Agric. Eng.* **2015**, *31*, 100–106. (In Chinese with English Abstract)
6. Su, Z.; Jacob, A.; Wen, J.; Roerink, G.; He, Y.; Gao, B.; Boogaard, H.; Diepen, C.V. Assessing relative soil moisture with remote sensing data: Theory, experimental validation, and application to drought monitoring over the North China Plain. *Phys. Chem. Earth Parts A/B/C* **2003**, *28*, 89–101. [[CrossRef](#)]
7. Jia, M.U.; Qiu, M.J.; Yu, G.U.; Ren, J.Q.; Liu, Y.; Jian, M.A. Applicability of five drought indices for agricultural drought evaluation in Jilin Province, China. *Chin. J. Appl. Ecol.* **2018**, *29*, 2624–2632. (In Chinese with English Abstract)

8. Anderson, M.C.; Zolin, C.A.; Sentelhas, P.C.; Hain, C.R.; Semmens, K.; Tugrul Yilmaz, M.; Gao, F.; Otkin, J.A.; Tetrault, R. The Evaporative Stress Index as an indicator of agricultural drought in Brazil: An assessment based on crop yield impacts. *Remote Sens. Environ.* **2016**, *174*, 82–99. [[CrossRef](#)]
9. Vilhar, U. Comparison of drought stress indices in beech forests: A modelling study. *iForest Biogeosciences For.* **2016**, *9*, 635–642. [[CrossRef](#)]
10. Shen, G.; Tian, G. Remote sensing monitoring of drought in Huanghe, Huaihe and Haihe plain based on GIS—the calculation of crop water stress index model. *Acta Ecol. Sin.* **2000**, *20*, 224–228. (In Chinese with English Abstract)
11. Kogan, F.N. Remote sensing of weather impacts on vegetation in non-homogeneous areas. *Int. J. Remote Sens.* **1990**, *11*, 1405–1419. [[CrossRef](#)]
12. Huang, J.X.; Zhuo, W.; Li, Y.; Huang, R.; Sedano, F.; Su, W.; Dong, J.W.; Tian, L.Y.; Huang, Y.B.; Zhu, D.H.; et al. Comparison of three remotely sensed drought indices for assessing the impact of drought on winter wheat yield. *Int. J. Digit. Earth* **2020**, *13*, 504–526. [[CrossRef](#)]
13. Venturin, A.Z.; Guimaraes, C.M.; de Sousa, E.F.; Filho, J.A.M.; Rodrigues, W.P.; Serrazine, D.A.; Bressan-Smith, R.; Marciano, C.R.; Campostrini, E. Using a crop water stress index based on a sap flow method to estimate water status in conilon coffee plants. *Agr. Water Manag.* **2020**, *241*, 106343. [[CrossRef](#)]
14. Hoffmann, H.; Jensen, R.; Thomsen, A.; Nieto, H.; Rasmussen, J.; Friberg, T. Crop water stress maps for entire growing seasons from visible and thermal UAV imagery. *Biogeoscience* **2016**, *13*, 6545–6563. [[CrossRef](#)]
15. Dangwal, N.; Patel, N.R.; Kumari, M.; Saha, S.K. Monitoring of water stress in wheat using multispectral indices derived from Landsat-TM. *Geocarto Int.* **2015**, *31*, 1–26. [[CrossRef](#)]
16. Yang, S.E.; Yan, N.N.; Bing-Fang, W.U. Advances in Agricultural Drought Monitoring by Remote Sensing. *Remote Sens. Inf.* **2010**, *32*, 103–109. (In Chinese with English Abstract)
17. Zhang, C. Spatial and Temporal Variations of Water Consumption for Major Grains Production in the Northern China Based on Remote Sensing and Statistical Data. Master's Thesis, Hebei Normal University, Shijiazhuang, China, 2014. (In Chinese with English Abstract)
18. McDaniel, R. Crop- and Location-Specific Drought Index for Agricultural Water Management: Development, Evaluation, and Forecasting. Ph.D. Thesis, Texas A&M University, Ann Arbor, MI, USA, 2015.
19. Zhang, Z.; Xu, W.; Shi, Z.; Qin, Q. Establishment of a Comprehensive Drought Monitoring Index Based on Multisource Remote Sensing Data and Agricultural Drought Monitoring. *IEEE J. STARS* **2021**, *14*, 2113–2126. [[CrossRef](#)]
20. Zhou, H.; Geng, G.; Yang, J.; Hu, H.; Sheng, L.; Lou, W. Improving Soil Moisture Estimation via Assimilation of Remote Sensing Product into the DSSAT Crop Model and Its Effect on Agricultural Drought Monitoring. *Remote Sens.* **2022**, *14*, 3187. [[CrossRef](#)]
21. Wang, Z.H.; Liu, J.D.; Liu, L.; Ding-Rong, W.U.; Qiu, M.J.; Feng, Y.D. Regional Agro-drought Simulation Based on Remote Sensing Technology. *Bull. Soil Water Conserv.* **2013**, *33*, 96–100, 122.
22. Gao, H.; Wood, E.F.; Jackson, T.J.; Drusch, M.; Bindlish, R. Using TRMM/TMI to Retrieve Surface Soil Moisture over the Southern United States from 1998 to 2002. *J. Hydrometeorol.* **2004**, *7*, 815–818. [[CrossRef](#)]
23. Escorihuela, M.J.; Chanzy, A.; Wigneron, J.P.; Kerr, Y.H. Effective soil moisture sampling depth of L-band radiometry: A case study. *Remote Sens. Environ.* **2010**, *114*, 995–1001. [[CrossRef](#)]
24. Li, X.; Zeng, Q.; Wang, X.; Huang, J.; Jiao, J. A soil moisture co-retrieval approach based on AMSR-E and ASAR data. *Acta Sci. Nat. Univ. Pekin.* **2016**, *52*, 902–910.
25. Wu, Z.; Lu, G.; Wen, L.; Lin, C.A.; Zhang, J.; Yang, Y. Thirty-five year (1971–2005) simulation of daily soil moisture using the variable infiltration capacity model over China. *Atmos. Ocean.* **2007**, *45*, 37–45. [[CrossRef](#)]
26. Manfreda, S.; Brocca, L.; Moramarco, T.; Melone, F. A physically based approach for the estimation of root-zone soil moisture from surface measurements. *Hydrol. Earth Syst. Sci.* **2014**, *18*, 1199–1212. [[CrossRef](#)]
27. Mcnider, R.T.; Handyside, C.; Doty, K.; Ellenburg, W.L.; Cruise, J.F.; Christy, J.R.; Moss, D.; Sharda, V.; Hoogenboom, G.; Caldwell, P. An integrated crop and hydrologic modeling system to estimate hydrologic impacts of crop irrigation demands. *Environ. Modell. Softw.* **2015**, *72*, 341–355. [[CrossRef](#)]
28. Yang, S.; Fang, S.; Wei, Y. Comparison of typical remote sensing drought indexes and their adaptability in agriculture. *Sci. Technol. Rev.* **2016**, *34*, 45–52. (In Chinese with English Abstract)
29. Siad, S.M.; Iacobellis, V.; Zdruli, P.; Gioia, A.; Stavi, I.; Hoogenboom, G. A review of coupled hydrologic and crop growth models. *Agr. Water Manag.* **2019**, *224*, 105746. [[CrossRef](#)]
30. Lu, G.; Liu, J.; Wu, Z.; He, H.; Xu, H.; Lin, Q. Development of a large-scale routing model with scale independent by considering the damping effect of sub-basins. *Water Resour. Manag.* **2015**, *29*, 5237–5253. [[CrossRef](#)]
31. Neitsch, S.; Arnold, J.; Kiniry, J.; Williams, J. *Soil and Water Assessment Tool Theoretical Documentation*; Texas A&M University: Ann Arbor, MI, USA, 2011.
32. Zhang, Y.; Wu, Z.; Singh, V.P.; He, H.; He, J.; Yin, H.; Zhang, Y. Coupled hydrology-crop growth model incorporating an improved evapotranspiration module. *Agr. Water Manag.* **2021**, *246*, 106691. [[CrossRef](#)]
33. Zhang, Y.; Wu, Z.; Singh, V.P.; Su, Q.; He, H.; Yin, H.; Zhang, Y.; Wang, F. Simulation of crop water demand and consumption considering irrigation effects based on Coupled Hydrology-Crop growth model. *J. Adv. Model. Earth Syst.* **2021**, *13*, e2020MS002360. [[CrossRef](#)]
34. China Meteorological Administration. *Grade of Agricultural Drought*; China Standards Press: Beijing, China, 2015.

35. Wu, Z.Y.; Lu, G.H.; Wen, L.; Lin, C.A. Reconstructing and analyzing China's fifty-nine year (1951–2009) drought history using hydrological model simulation. *Hydrol. Earth Syst. Sci. Discuss.* **2011**, *8*, 2881–2894. [[CrossRef](#)]
36. Mao, Y. Regional Drought Analysis and Risk Assessment Based on Simulated Soil Moisture in Jiangsu. Master's Thesis, Hohai University, Nanjing, China, 2017. (In Chinese with English Abstract)
37. Palmer, W.C. *Meteorological Drought*; U.S. Weather Bureau: Washington, DC, China, 1965.
38. Mao, Y.; Wu, Z.; He, H.; Lu, G.; Xu, H.; Lin, Q. Spatio-temporal analysis of drought in a typical plain region based on the Soil Moisture Anomaly Percentage Index. *Sci. Total Environ.* **2016**, *576*, 752–765. [[CrossRef](#)] [[PubMed](#)]
39. Lu, G.; Wu, Z.; He, H. *Dynamic Monitoring and Prediction of Drought in a Large Scale*; Science Press: Beijing, China, 2021. (In Chinese)
40. Bao, Y.; Meng, C.; Shen, S.; Qiu, X.; Gao, P.; Liu, C. Analysis on characteristics of a typical drought event in Jiangsu Province. *Acta Ecol. Sin.* **2011**, *31*, 6853–6865. (In Chinese with English Abstract)
41. Ren, Z.; Zou, F.; Yu, Y. *Daily Data Set of Surface Climatic Data in China*; National Meteorological Information Center China Meteorological Data: Beijing, China, 2020.
42. Farr, T.G.; Kobrick, M. Shuttle radar topography mission produces a wealth of data. *Eos Trans. Am. Geophys. Union* **2000**, *81*, 583–585. [[CrossRef](#)]
43. Pekel, J.F.; Cottam, A.; Gorelick, N.; Belward, A.S. High-resolution mapping of global surface water and its long-term changes. *Nature* **2016**, *540*, 418–422. [[CrossRef](#)] [[PubMed](#)]
44. Reynolds, C.A.; Jackson, T.J.; Rawls, W.J. Estimating soil water-holding capacities by linking the Food and Agriculture Organization Soil map of the world with global pedon databases and continuous pedotransfer functions. *Water Resour. Res.* **2000**, *36*, 3653–3662. [[CrossRef](#)]
45. Saxton, K.E.; Rawls, W.J.; Romberger, J.S.; Papendick, R.I. Estimating generalized soil-water characteristics from Texture. *Soil Sci. Soc. Am. J.* **1986**, *50*, 1031–1036. [[CrossRef](#)]
46. Wu, Z.; Lu, G.; Zhang, J.; Yang, Y. Simulation of daily soil moisture using VIC Model. *Sci. Geogr. Sin.* **2007**, *27*, 359–363. (In Chinese with English Abstract)
47. Lu, G.H.; Zhang, J.; Wu, Z.Y.; He, H. Parameter gridding formulas of VIC Model in Southern region of China and effect verification. *Water Resour. Power* **2013**, *31*, 13–17. (In Chinese with English Abstract)
48. Rajib, M.A.; Merwade, V.; Yu, Z. Multi-objective calibration of a hydrologic model using spatially distributed remotely sensed/in-situ soil moisture. *J. Hydrol.* **2016**, *536*, 192–207. [[CrossRef](#)]
49. Wang, B. The Influence of Different Water Supplied on Root Morphology and Water Uptake Ability in Winter Wheat. Ph.D. Thesis, Taiyuan University of Technology, Taiyuan, China, 2017. (In Chinese with English Abstract)
50. You-Jie, W.U.; Wei, Z.H.; Tai-Sheng, D.U. Characteristics of Stable Hydrogen and Oxygen Isotopes in Soil Water under Alternate Partial Root-zone Furrow Irrigation. *J. Irrig. Drain.* **2014**, *33*, 251–255. (In Chinese with English Abstract)
51. Jiang, X. Research on the Maize Rhizosphere Regulation Mechanism under the Condition of Mulching and Construction of Root Water Uptake Model. Master's Thesis, Northeast Agricultural University, Harbin, China, 2013. (In Chinese with English Abstract)
52. Jiangsu Provincial Water Resources Department. *Jiangsu Water Conservancy Yearbook*; Hohai University Press: Nanjing, China, 1989–2020.
53. Sayago, S.; Ovando, G.; Bocco, M. Landsat images and crop model for evaluating water stress of rainfed soybean. *Remote Sens. Environ.* **2017**, *198*, 30–39. [[CrossRef](#)]
54. Wu, Q.; Mei, J. *Severe Meteorological Drought Continues to Occur in Most Areas of Jiangsu Province*; Jiangsu Now: Nanjing, China, 2019; Available online: http://www.legaldaily.com.cn/locality/content/2019-11/19/content_8051184.htm (accessed on 19 November 2019). (In Chinese)